Kinetic and Crystallographic Studies on the Active Site Arg289Lys Mutant of Flavocytochrome b_2 (Yeast L-Lactate Dehydrogenase)†

Christopher G. Mowat,‡,§ Isabelle Beaudoin,§,|| Rosemary C. E. Durley,§,⊥ John D. Barton,⊥ Andrew D. Pike,‡ Zhi-wei Chen,⊥ Graeme A. Reid,@ Stephen K. Chapman,‡ F. Scott Mathews,*,⊥ and Florence Lederer||

Department of Chemistry, University of Edinburgh, West Mains Road, Edinburgh EH9 3JJ, Scotland, U.K., Laboratoire d'Enzymologie et Biochimie Structurales, Centre National de la Recherche Scientifique, 91198 Gif-sur-Yvette Cedex, France, Department of Biochemistry and Molecular Biophysics, Washington University School of Medicine, St. Louis, Missouri 63110, and Institute of Cell and Molecular Biology, University of Edinburgh, Mayfield Road, Edinburgh EH9 3JR, Scotland, U.K.

Received November 9, 1999

ABSTRACT: Flavocytochrome b_2 from *Saccharomyces cerevisiae* couples L-lactate dehydrogenation to cytochrome *c* reduction. The crystal structure of the native yeast enzyme has been determined [Xia, Z.-X., and Mathews, F. S. (1990) *J. Mol. Biol. 212*, 837−863] as well as that of the sulfite adduct of the recombinant enzyme produced in *Escherichia coli* [Tegoni, M., and Cambillau, C. (1994) *Protein Sci. 3*, 303−313]; several key active site residues were identified. In the sulfite adduct crystal structure, Arg289 adopts two alternative conformations. In one of them, its side chain is stacked against that of Arg376, which interacts with the substrate; in the second orientation, the R289 side chain points toward the active site. This residue has now been mutated to lysine and the mutant enzyme, R289K-b_2, characterized kinetically. Under steady-state conditions, kinetic parameters (including the deuterium kinetic isotope effect) indicate the mutation affects k_{cat} by a factor of about 10 and k_{cat}/K_M by up to nearly 10^2. Pre-steady-state kinetic analysis of flavin and heme reduction by lactate demonstrates that the latter is entirely limited by flavin reduction. Inhibition studies on R289K-b_2 with a range of compounds show a general rise in K_i values relative to that of wild-type enzyme, in line with the elevation of the K_M for L-lactate in R289K-b_2; they also show a change in the pattern of inhibition by pyruvate and oxalate, as well as a loss of the inhibition by excess substrate. Altogether, the kinetic studies indicate that the mutation has altered the first step of the catalytic cycle, namely, flavin reduction; they suggest that R289 plays a role both in Michaelis complex and transition-state stabilization, as well as in ligand binding to the active site when the flavin is in the semiquinone state. In addition, it appears that the mutation has not affected electron transfer from fully reduced flavin to heme, but may have slowed the second intramolecular ET step, namely, transfer from flavin semiquinone to heme b_2. Finally, the X-ray crystal structure of R289K-b_2, with sulfite bound at the active site, has been determined to 2.75 Å resolution. The lysine side chain at position 289 is well-defined and in an orientation that corresponds approximately to one of the alternative conformations observed in the structure of the recombinant enzyme−sulfite complex [Tegoni, M., and Cambillau, C. (1994) *Protein Sci. 3*, 303−313]. Comparisons between the R289K-b_2 and wild-type structures allow the kinetic results to be interpreted in a structural context.

Flavocytochrome b_2 (L-lactate:cytochrome *c* oxidoreductase, EC 1.1.2.3) from the yeast *Saccharomyces cerevisiae* is a soluble component of the mitochondrial intermembrane space (*1*), where it couples L-lactate dehydrogenation to cytochrome *c* reduction (*2*). The DNA encoding *S. cerevisiae* flavocytochrome b_2 has been cloned and expressed at a high level in *Escherichia coli* (*3*). The enzyme is a homotetramer with a subunit M_r of 57.5 kDa (*4*). The structures have been determined for the native enzyme from *S. cerevisiae* crystallized in the presence of lactate (*5*) and for the sulfite adduct of the recombinant enzyme expressed in *E. coli* (*6*). These are isostructural and clearly show that each subunit is composed of two distinct domains. The smaller of these is the N-terminal cytochrome domain containing protoheme IX (residues 1−99), and the larger is the C-terminal domain containing noncovalently bound flavin mononucleotide (FMN).[1]

In light of previous functional studies, possible roles in the catalysis of substrate dehydrogenation were assigned to various side chains observed to lie close to the flavin in the crystal structure (*7*). These residues occupy identical positions in the glycolate oxidase crystal structure (*8*); furthermore,

† This work was supported by NIH Grant GM-20530 (F.S.M.), by the CNRS and the Royal Society (Program "Alliance"), and via a Caledonian Research Foundation Scholarship and Carnegie Grant to C.G.M.

* To whom correspondence should be addressed. E-mail: mathews@biochem.wustl.edu. Telephone: (314) 362 10 80.

‡ Department of Chemistry, University of Edinburgh.

§ These authors contributed equally to the work.

|| Centre National de la Recherche Scientifique.

⊥ Washington University School of Medicine.

@ Institute of Cell and Molecular Biology, University of Edinburgh.

[1] Abbreviations: FMN, flavin mononucleotide; $FMNH^-$, anion of FMN hydroquinone; $FMN^\bullet$, anion of FMN semiquinone; NCS, non-crystallographic symmetry; rms, root-mean-square.

10.1021/bi9925975 CCC: $19.00
Published on Web 03/03/2000

they were found conserved, with one exception, in the sequences of related enzymes such as lactate dehydrogenase from *E. coli* (*9*), lactate monooxygenase from *Mycobacterium smegmatis* (*10*), lactate oxidase from *Aerococcus viridans* (*11*), long-chain 2-hydroxy acid oxidase from rat kidney (*12*), and mandelate dehydrogenases from *Pseudomonas putida* (*13*) and *Rhodotorula graminis* (*14*).The catalytic roles of many of these active site residues have been probed by site-directed mutagenesis (*15*).

One residue close to the active site, but which has until now not been studied in detail, is Arg289. From the crystal structure, Arg289 would appear to have a dual role. First, its side chain is stacked above that of Arg376 (at ~3.7 Å), a key residue thought to be involved in Michaelis complex formation and catalysis; second, it appears to take part in an interdomain interaction by hydrogen bonding, via a water molecule, to one of the heme propionates (*5*). In addition, in the crystal structure of recombinant flavocytochrome b_2, which has a sulfite ion bound at position N5 of the FMN, two different conformations are displayed by Arg289, suggesting some degree of conformational flexibility (*6*). One explanation for the second conformation is an electrostatic attraction between Arg289 and the bound sulfite. As a consequence of these structural observations, we might expect Arg289 to influence both substrate binding and catalysis and also possibly interdomain electron transfer.

To probe more fully the role of this residue, we have constructed the Arg289Lys mutant form of flavocytochrome b_2 (R289K-b_2). In this paper, we report a combined kinetic and crystallographic characterization of this mutant enzyme.

MATERIALS AND METHODS

DNA Manipulation, Strains, and Growth. Site-directed mutagenesis was performed by the Kunkel method of nonphenotypic selection (*16*) using the oligonucleotide H3100 (TTAGGTCAAAAAGAAAAAGAT) (Oswel DNA Service). Standard methods for growth of *E. coli*, plasmid purification, DNA manipulation, and transformation were performed as described previously (*17*). *E. coli* strain AR120 was used for expression of mutant flavocytochrome b_2.

Enzyme Preparation. R289K mutant flavocytochrome b_2 expressed in *E. coli* was isolated from cells which had been stored at −20 or −80 °C, using a previously reported purification procedure (*3*). Purified enzyme samples were stored either under nitrogen at 4 °C as precipitates from a 70% saturated $(NH_4)_2SO_4$ solution (short-term storage), as concentrated solutions at −80 °C, or as snap-frozen enzyme drops in liquid nitrogen (long-term storage). Prior to freezing or after thawing, the enzyme was desalted on a Sephadex G25 gel filtration column equilibrated with 0.1 M K^+/Na^+ phosphate buffer and 1 mM EDTA (pH 7). This same buffer was used throughout.

Steady-State Kinetics. Steady-state kinetic analyses were carried out at 30 °C using a Uvikon 930 spectrophotometer. L-Lactate dehydrogenase activity was assayed using both ferricyanide and cytochrome *c* (horse heart, type VI, Sigma) as electron acceptors, at the concentrations indicated in the tables or as varying substrates. Reduction of ferricyanide was monitored at 420 nm as described previously (*18*), and reduction of cytochrome *c* was monitored at 550 nm using published molar extinction coefficients (*19*). Kinetic isotope effects were measured using L-[2-^{2}H]lactate prepared and purified as previously described (*20*). The purity of the L-[2-^{2}H]lactate was determined by ^{1}H NMR spectroscopy. For inhibitor studies, around seven different inhibitor concentrations and seven L-lactate concentrations were used in general for each experiment. Ferricyanide (2 mM) was the electron acceptor used in this case. K_i values were determined from double-reciprocal plots, except for pyruvate, for which Dixon plots were used.

Pre-Steady-State Kinetics. Stopped-flow experiments were carried out using an Applied Photophysics DX.17 MV stopped-flow spectrophotometer. Analysis of kinetic data was performed using the instrument software. FMN and b_2-heme reduction were monitored by following absorbance changes at 438.3 and 557 nm, respectively (*21*).

Crystallography. Crystals of R289K-b_2 were grown by the sitting drop vapor diffusion method. A 5 μL aliquot of protein [8 mg/mL in 10 mM Tris-HCl buffer (pH 7.5), $I = 0.10$] was mixed with an equal volume of precipitant consisting of 20 mM MES buffer [2-(*N*-morpholino)ethanesulfonic acid] (pH 6.5), 50 mM sodium sulfite, and 12% PEG 4000 (polyethylene glycol). Crystals up to 0.2 mm × 0.2 mm × 0.1 mm grew in 3−5 days. If allowed to remain in the sitting drop, the crystals lost color and became rubber-like over the course of several days. For data collection, crystals were flash-frozen by briefly exposing them (ca. 2 min) to an artificial mother liquor containing the same precipitant with 25% MPD (2-methyl-2,4-pentanediol), mounting in a nylon loop, and quickly placing them in a 100 K nitrogen gas stream.

X-ray data were recorded from a single crystal at 100 K on a Rigaku R-axis IV image plate detector using a Ni-filtered, mirror-focused X-ray beam obtained from a Rigaku RU200 X-ray generator operated at a power of 5 keV. The crystal was trigonal, in space group $P3_221$, with the following unit cell parameters: $a = b = 163.0$ Å, $c = 112.2$ Å [about 1−1.5% smaller than native crystals assessed at room temperature (*5*)] $\alpha = \beta = 90°$, and $\gamma = 120°$. Spot integration and data scaling were carried out using HKL (*22*). Thirty frames of data, each 1° wide and 4 h in duration, yielded a data set that was 80% complete overall[2] to 2.75 Å resolution with an R_{merge}[3] of 0.078. The data collection statistics are summarized in Table 1.

Structure factor calculations, rigid body and simulated annealing refinement, and other crystallographic calculations were carried out using X-plor (*23*) and CNS (*24*). Model building and analysis of the structure were carried out on a Silicon Graphics workstation using Turbo-Frodo (*25*).

RESULTS

The mutant enzyme was expressed and purified from *E. coli* in yields similar to those of the wild-type protein. When the flavin content was analyzed using difference spectra in the presence of sulfite, as described previously (*26*), some preparations were found to have a flavin to heme stoichiometry lower than 1, as already observed for a few active site mutant flavocytochromes b_2 (*27*). The specific activity,

[2] After 30 frames of data collection, the crystal was lost as the result of an instrument failure.

[3] The definitions of R_{merge}, R, and R_{free} are given in the footnotes of Table 1.

Table 1: Data Collection and Refinement Statistics for the R289K Mutant of Flavocytochrome b_2

data collection	
resolution range (all/outer) (Å)	30.0−2.75/2.87−2.75
no. of reflections	36062
completeness (all/outer) (%)	80.8/75.2
R_{merge} (all/outer) (%)[a]	7.8/41.6
$(I)/\sigma(I)$ (all/outer)[b]	7.8/1.3
redundancy (all/outer)	1.7/1.3
refinement	
resolution range (all/outer) (Å)	500.0−2.75 (2.88/2.75)
R (all/outer)[c]	20.7/29.9
R_{free} (all/outer)[c,d]	22.1/33.8
no. of protein atoms (non-H)	3154
protein $\langle B \rangle$ (Å^2)	39
no. of solvent molecules	64
solvent $\langle B \rangle$ (Å^2)	28
rms deviation for bond lengths (Å^2)	0.012
rms deviation for bond angles (deg)	1.6
rms deviation for dihedral angles (deg)	24.5
rms deviation for improper dihedral angles (deg)	1.67

[a] $R_{merge} = \Sigma_h\Sigma_i|I(h) - I_i(h)|/\Sigma_h\Sigma_i I_i(h)$, where $I_i(h)$ and $I(h)$ are the ith and mean measurement of reflection h, respectively. [b] $I/\sigma(I)$ is the average signal-to-noise ratio for merged reflection intensities. [c] $R = \Sigma_h|F_o - F_c|/\Sigma_h F_o$, where F_o and F_c are the observed and calculated structure factor amplitudes of reflection h, respectively. [d] R_{free} is the test reflection data set, about 5% selected randomly for cross validation during crystallographic refinement (*52*).

when expressed per flavin, was identical to that of the fully flavinylated enzyme.

Steady-State Kinetic Parameters. Steady-state kinetic parameters for lactate were previously determined in Tris-HCl buffer (I = 0.1, pH 7.5, and 25 °C) (*28*) and were compared with data for the wild-type enzyme determined in the same buffer (*29*). Table 2 now presents values determined in 0.1 M phosphate buffer (pH 7 and 30 °C). With ferricyanide as an acceptor, the k_{cat} value for the mutant enzyme is lower than the wild-type one by about an order of magnitude, and the catalytic efficiency (k_{cat}/K_M) by about 2 orders of magnitude. The deuterium kinetic isotope effect is similar to that of the wild-type enzyme; these results indicate that the mutation has affected C(2)−H bond cleavage, the first step in the catalytic cycle, and that R289 participates in both Michaelis complex and transition-state stabilization. The previously published values obtained in Tris buffer (pH 7.5 and 25 °C) had led to similar conclusions.

With cytochrome *c* as an acceptor, k_{cat} values appear somewhat lower than the corresponding value for ferricyanide reduction and, as with ferricyanide, are lower by an order of magnitude than those for cytochrome *c* reduction by the wild-type enzyme (Table 2). Cytochrome *c* is reduced only by heme b_2 (Scheme 1), whereas ferricyanide, in the wild-type enzyme case under normal conditions, is also reduced by the flavin semiquinone, but not by two-electron-reduced flavin (*30*). The K_M^{app} value of the wild-type enzyme for ferricyanide is very low; it has been proposed that an increase in this value is a sign that ferricyanide takes an electron also from the fully reduced flavin (*30*). This has been verified for the isolated recombinant flavodehydrogenase domain (*31*) and for a number of mutant enzymes with reduced rates of electron transfer from flavin to heme (see, for example, ref *29*). With R289K-b_2, the ferricyanide K_M^{app} value was 30 μM in phosphate buffer, similar to that for the wild-type enzyme (*32*). At this stage, therefore, the steady-state kinetic parameters for lactate as a substrate do not give any indication that the rate of $FMNH^-$ to heme electron transfer has been strongly affected by the mutation.

Scheme 1

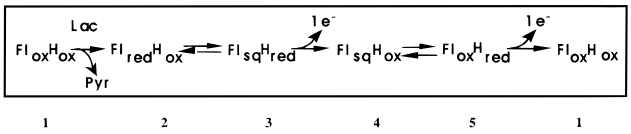

As an example of a second substrate, L-phenyllactate was also investigated. The results are presented in Table 3. The k_{cat} values of mutant and wild-type enzymes differ by a factor of only 2; in view of their low value, it can be surmised that flavin reduction is totally rate-determining in the catalytic cycle with this substrate and, therefore, that the K_M value is a K_d value. Thus, the mutation has affected the binding of phenyllactate, a poor substrate, as well as that of the physiological substrate. The k_{cat}/K_M value is decreased (by about an order of magnitude), thus indicating that for this substrate the mutation also destabilizes the transition state.

Pre-Steady-State Kinetics. Preliminary stopped-flow data in Tris-HCl buffer have been reported in ref *28*. Stopped-flow data have now been obtained in 0.1 M phosphate buffer and 1 mM EDTA (pH 7 and 30 °C). Figure 1a shows the lactate concentration dependence of flavin and heme reduction rates; Table 4 presents the derived kinetic parameters. Before these are discussed, a number of comments are in order. Stopped-flow kinetic traces were generally fitted to double-exponential functions, due to the biphasic kinetic behavior which has been proposed to result from a slow intersubunit electron transfer between two single-electron-reduced subunits in the tetramer, so as to regenerate one fully oxidized flavin per two subunits and to allow entrance of four more reducing equivalents for complete tetramer reduc-

Table 2: Steady-State Kinetic Parameters for L-Lactate[a]

	L-[2-^{1}H]lactate						L-[2-^{2}H]lactate			
	ferricyanide			cytochrome *c*			ferricyanide			
	k_{cat} (s^{-1})	K_M (mM)	k_{cat}/K_M (mM^{-1} s^{-1})	k_{cat} (s^{-1})	K_M (mM)	k_{cat}/K_M (mM^{-1} s^{-1})	k_{cat} (s^{-1})	K_M (mM)	k_{cat}/K_M (mM^{-1} s^{-1})	^DV
wild type[b]	270 ± 30	0.49 ± 0.10	551 ± 174	155 ± 15	0.29 ± 0.05	534 ± 144	65 ± 22	0.50 ± 0.23	130 ± 104	4.5 ± 1.1
R289K	20.6 ± 2.0	3.2 ± 0.4	6.4 ± 1.4	16.5 ± 0.4	*c*	*c*	4.7 ± 0.4	4.3 ± 0.4	1.1 ± 0.2	4.4 ± 0.8

[a] Assays were carried out in 0.1 M Na^+/K^+ phosphate buffer and 1 mM EDTA (pH 7 and 30 °C). The ferricyanide concentration was 1 mM; activity units are moles of substrate oxidized per second per mole of subunit. [b] The values for lactate and deuteriolactate are taken from refs *32* and *38*. [c] These experiments were carried out in 40 mM lactate at varying cytochrome *c* concentrations. The K_M^{app} for cytochrome *c* was 74 (±8) μM, similar to that for the wild-type enzyme (*32*).

Table 3: Steady-State Kinetic Parameters for L-Phenyllactate[a]

	k_{cat} (s^{-1})	K_M (mM)	k_{cat}/K_M (mM^{-1} s^{-1})
wild type[b]	12.4 ± 0.7	0.22 ± 0.02	56 ± 6
R289K	6.0 ± 0.2	1.43 ± 0.05	4.2 ± 0.2

[a] Assays were carried out in 0.1 M Na^+/K^+ phosphate buffer and 1 mM EDTA (pH 7 and 30 °C). The ferricyanide concentration was 2 mM. Activity units are moles of substrate oxidized per second per mole of subunit. [b] Taken from ref *35*.

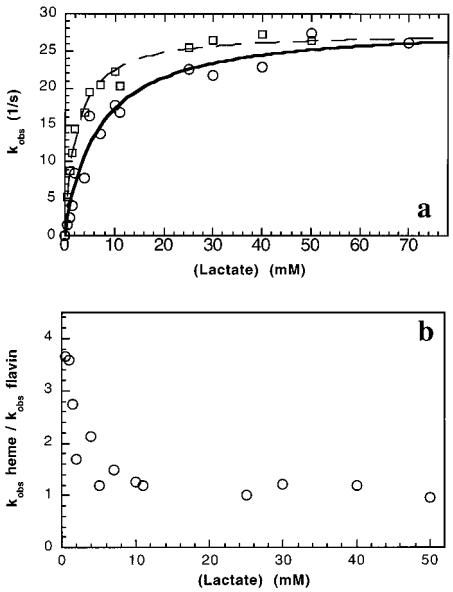

FIGURE 1: Lactate concentration dependence of flavin and heme reduction rates: (a) flavin reduction (○) and heme reduction (□). k_{obs} values are those of the fast phase, except for flavin at low lactate concentrations (up to 1.5 mM included), for which the traces could only be fitted with a monoexponential equation (see the text). The figure shows the combined data from two independent experiments. (b) Ratio of k_{obs} values taken from part a as a function of lactate concentration.

tion (*20*, *21*). As this second phase is irrelevant to the catalytic cycle, only the figures for the first fast phase are presented in Table 4. With R289K-b_2, however, at the lower lactate concentrations (up to 1.5 mM), traces for flavin could only be fitted, or better fitted, with a single-exponential function. Furthermore, Figure 1a indicates that flavin reduction rates are generally lower than heme reduction rates, except at the higher concentrations, where they become similar (see also Table 4). This seems at first sight paradoxical, since flavin is the immediate heme reductant (Scheme 1). However, similar deviations from expectations (monoexponential behavior and slower flavin reduction than heme reduction) were observed previously in stopped-flow studies with deuteriolactate (i.e., at low rates of electron entry) with the proteolytically nicked form of the wild-type enzyme (Morton enzyme), which is 2−2.5-fold slower than the intact form (*20*). The results were rationalized in the following way (*33*). At low reduction rates, flavin reduction by the substrate undergoes competition with its reoxidation through the intersubunit electron reshuffling mentioned above. Figure 1b gives the ratio of heme to flavin reduction rates as a function of substrate concentration, showing a marked increase in this ratio at lower lactate concentrations, as described in ref *20*. In that paper, however, the ratio was below 1 for most of the rate range, indicating that heme reduction by flavin in the wild-type enzyme is not extremely fast relative to flavin reduction by substrate. For R289K-b_2, in contrast, the ratio reaches the value of 1 within error at saturation, indicating that heme reduction by $FMNH^-$ is entirely limited by flavin reduction itself. These results are the first ones, obtained with a mutant flavocytochrome b_2, which prove the correctness of the interpretation given by Pompon et al. (*20*) of the paradoxical results of the stopped-flow reduction kinetics at low rates of electron entry. They support the contention that the flavin reduction rate of slow mutant flavocytochromes b_2 cannot be studied using rapid kinetics (see, for example, ref *34*).

The kinetic parameters for R289K-b_2 cannot be compared directly to the values for the wild-type enzyme in the same buffer, since these were acquired at 5 °C (*32*) (Table 4). The comparison with the steady-state parameters obtained at 30 °C is however illuminating, but further discussion is deferred until later.

Inhibition Studies. A variety of different inhibitors and substrate analogues were employed to characterize inhibition in R289K-b_2, and investigate any alteration in binding at the active site as a result of the mutation. Inhibitors that were used were sulfite, D-lactate, L-mandelate, oxalate, and pyruvate. Sulfite is known to form a rapidly reversible covalent adduct with the flavin, by adding to the N5 position of the oxidized prosthetic group; sulfite thus behaves as a competitive inhibitor in steady-state kinetic assays (*26*). Table 5 shows no alteration in the sulfite dissociation constant for R289K-b_2 with respect to the wild-type enzyme. D-Lactate and mandelate both behave as strictly competitive inhibitors for R289K-b_2 as they do for the wild-type enzyme (*26*, *35*) but with a somewhat decreased affinity for the mutant enzyme (Table 5). Oxalate, on the other hand, behaves as a mixed-type inhibitor for the wild-type enzyme (*26*), but as a strictly competitive one toward R289K-b_2 (Figure 2), with a somewhat decreased affinity compared to the kinetically and spectroscopically determined values for the wild-type enzyme. As for pyruvate, it is known to exhibit a complex kinetic behavior toward the wild-type enzyme; in Dixon

Table 4: Pre-Steady-State Kinetic Parameters of R289K-b_2 Prosthetic Group Reduction

	flavin reduction			heme reduction		
	k_{red}^F (s^{-1})	K_d^{app} (mM)	k_{red}^F/K_d^{app} (mM^{-1} s^{-1})	k_{red}^H (s^{-1})	K_d (mM)	k_{red}^H/K_d (mM^{-1} s^{-1})
wild type[a]	144	0.89	162	108	0.54	200
R289K[b]	28.5 ± 1.4	6.7 ± 1.1	3.8 ± 0.8	27.6 ± 0.6	2.2 ± 0.2	12.5 ± 1.4

[a] Results taken from ref *32*. The buffer was the same as for R289K-b_2, but the temperature was 5 °C. [b] All experiments were carried out in Na^+/K^+ phosphate buffer and 1 mM EDTA (pH 7 and 30 °C). For flavin observation, the enzyme concentration was 10 μM, and for heme observation, it was 5 μM. The kinetics were recorded for 2.2 s. Stopped-flow data were analyzed as described in Materials and Methods. Values of k are given in terms of the number of prosthetic groups reduced per second. k_{red}^F and k_{red}^H are the rate constants for the fast phases of flavin and heme reduction, respectively.

Table 5: Inhibition of R289K and Wild-Type Flavocytochrome b_2[a]

inhibition	K_i (mM)	wild-type inhibition type	K_i (mM)	R289K inhibition type
sulfite	$(1.4 \pm 0.5) \times 10^{-3}$	competitive[b]	$(1.9 \pm 0.6) \times 10^{-3}$	competitive
D-lactate	1.4 ± 0.5	competitive[b]	6.7 ± 0.7	competitive
L-mandelate	0.26 ± 0.3	competitive[c]	1.0 ± 0.3	competitive
pyruvate	3	competitive[d]	39.2 ± 2.9	competitive
	30	noncompetitive[d]		
oxalate	0.3 ± 0.1	mixed[e]	0.95 ± 0.25	competitive

[a] Assays were carried out in Na^+/K^+ phosphate buffer and 1 mM EDTA (pH 7 and 30 °C). The ferricyanide concentration was 2 mM. [b] Taken from ref *26*. [c] Taken from ref *35*. [d] For the wild-type enzyme, pyruvate displays noncompetitive inhibition in Dixon plots at high concentrations, but below 10 mM, inhibition is competitive (*26*). [e] The figure of 0.3 mM is obtained from secondary plots of slope values taken from Figure 4 of ref *26*. Difference spectral titrations reported in the same paper gave a K_d of 0.5 mM for the oxidized enzyme−oxalate complex.

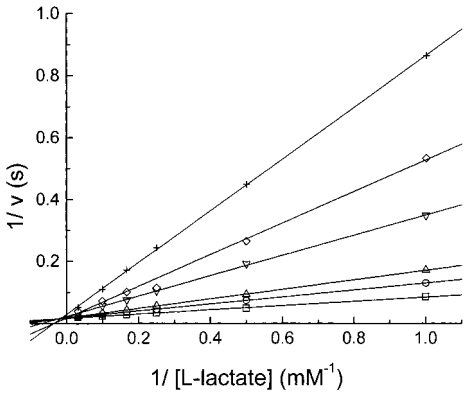

FIGURE 2: Double-reciprocal plot for oxalate inhibition of R289K-b_2. The oxalate concentrations are 0 (□), 0.5 (○), 1 (△), 3 (▽), 5 (◇), and 10 mM (+). Experiments were carried out at 30 °C in 0.1 M phosphate buffer (pH 7) in the presence of 2 mM ferricyanide.

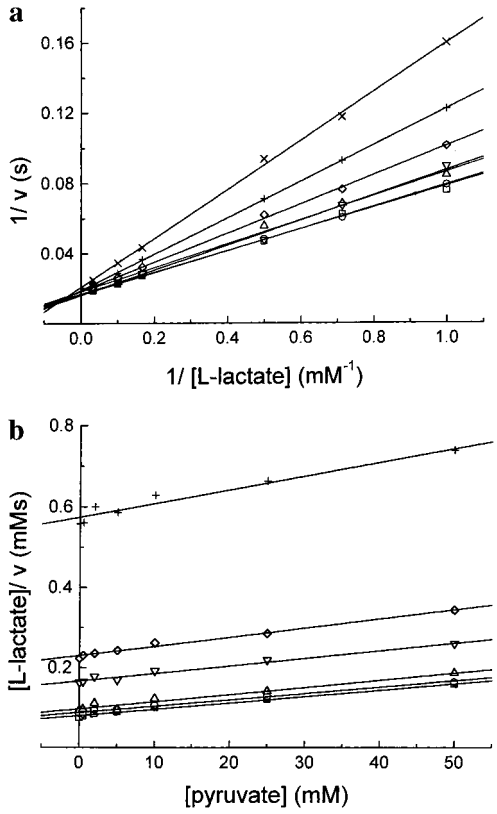

FIGURE 3: Pyruvate inhibition of R289K-b_2. (a) Double-reciprocal plot. The pyruvate concentrations are 0 (□), 0.5 (○), 2 (△), 5 (▽), 10 (◇), 25 (+), and 50 mM (×). For experimental conditions, see the legend of Figure 2. (b) Cornish−Bowden plot. The data are taken from panel a. Lactate concentration are 1 (□), 1.4 (○), 2 (△), 6 (▽), 10 (◇), and 30 mM (+).

plots, two slopes were observed, one at low concentrations (less than ~10 mM) corresponding to competitive inhibition and the other one at higher concentrations (>10 mM) corresponding to noncompetitive inhibition, with K_i and K_i' values of 3 and 30 mM, respectively, while differential spectrophotometric titration gave a K_d value of 30 mM (*26*). In contrast, with R289K-b_2, both the double-reciprocal plot and the Dixon plot appeared to indicate competitive inhibition, or possibly mixed inhibition (see Figure 3a for a representative experiment). To clarify this point, a further plot of [L-lactate]/v versus [pyruvate] was created according to the method of Cornish-Bowden (*36*) (Figure 3b). In this case, competitive inhibition is indicated by the presence of parallel lines for each substrate concentration. Thus, for both oxalate and pyruvate, the R289K mutation results in a modification of the inhibition pattern to simple competitive behavior. In addition, the inhibition by excess substrate was tested since it can be observed for the wild-type enzyme above about 25 mM L-lactate. With ferricyanide as an acceptor under the same experimental conditions (*32*), R289K-b_2 did not manifest any observable inhibition up to 130 mM substrate. These changes in inhibition patterns will be considered in the Discussion.

Crystallography. (1) Structure Analysis and Refinement. The flavocytochrome b_2 native structure (*5*) was used as a starting point for refinement and, after initial scale factor adjustment, gave R and R_{free}[3] values of 0.373 and 0.373, respectively, in the resolution range of 10−2.7 Å. At this early stage of refinement using X-plor (*23*), strong electron density was observed above the N5 atom of the FMN, indicating that a sulfite ion was covalently bound to the nitrogen atom. The structure of recombinant flavocytochrome b_2 containing sulfite bound to the FMN (*6*) was then substituted for the yeast structure; Arg289 was replaced by alanine, and initial positional refinement was carried out, giving R and R_{free} values of 0.251 and 0.348, respectively. Five rounds of simulated annealing and positional and group temperature factor refinement for the main chain and side chain atoms of each residue, alternated with model building, reduced R and R_{free} to 0.201 and 0.281, respectively. Halfway through this refinement, the coordinates for the cytochrome domain of subunit 1 (up to residue 101) were omitted since no interpretable electron density could be identified for the domain. Residue 289 was then changed to lysine, fit to the electron density, and water molecules were gradually introduced into the model during the course of four cycles of positional refinement, *B*-factor refinement, and model building.

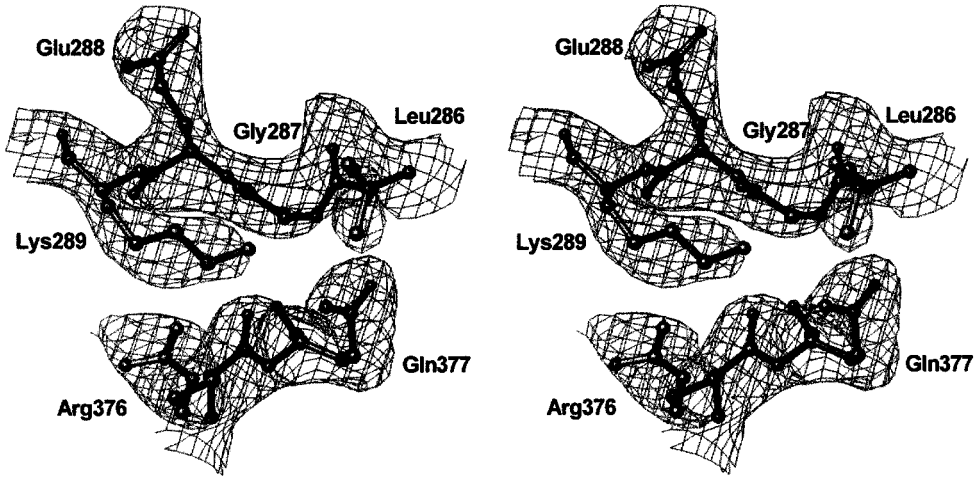

FIGURE 4: Stereodiagram of the electron density map of the R289K mutant of flavocytochrome b_2. The map was computed using Fourier coefficients ($2F_o - F_c$), where F_o and F_c are the observed and calculated structure factors, respectively, the latter based on the final model. The density only for residues Leu286−Lys289 and Arg376 and Gln377 is shown. The contour level is 1.25σ, where σ is the rms electron density. This diagram was generated using TURBO-FRODO (*25*).

At this point, strict noncrystallographic symmetry (NCS) constraints were introduced, reducing the number of refinable parameters to those of just one flavin-binding domain, and further refinement was carried out using CNS (*24*). This was done because of the relatively incomplete data coverage and limited resolution of the data collection. The final model consists of 388 residues in each subunit (residues 99−297 and 320−511),[4] one molecule each of FMN and sulfite, and 64 water molecules. The final R and R_{free} are 0.209 and 0.227, respectively, for 28 365 reflections with $F > \sigma(F)$ in the resolution range of 100.0−2.75 Å; the root-mean-square (rms) deviations for bond lengths and angles from ideal values are 0.012 Å and 1.65°, respectively. The refinement statistics are summarized in Table 1. Analysis of the Ramachandran plot using PROCHECK (*37*) shows that 339 non-glycine and non-proline residues (99.4%) are in the most favored and additionally allowed regions and two residues are in disallowed regions.

(2) Structure of the R289K Mutant Flavocytochrome b_2. The most notable feature of R289K-b_2 is the clear presence of the lysine side chain at position 289 (Figure 4). Its orientation is well-defined and differs from that of the arginine side chain that it replaces in the native yeast and recombinant wild-type forms of the enzyme (see below). A second important feature of the R289K-b_2 structure is the absence of the cytochrome domain in both subunits. The first residue in either subunit that could be fitted to the density was Thr102. In the native yeast structure (*5*), the cytochrome domain (residues 1−99) is absent in subunit 2, but present in subunit 1, although less well ordered than the flavin-binding domain and having generally higher temperature factors. The absence of the ordered cytochrome domain was first detected by its very high B-factors (average $B = 88$ vs 25 Å^2 for the flavin-binding domain) during initial refinement, and the lack of interpretable electron density even at the heme. Further evidence of cytochrome disorder in both domains comes from the behavior of Phe325. In the native yeast and recombinant sulfite-bound structures (*5*, *6*), Phe325 protrudes into solution in subunit 2 and is poorly ordered with B-factors of 60−80 Å^2. In subunit 1 of these structures, the side chain is tucked onto the surface of the flavin-binding domain and has low B-factors (25−35 Å^2). If the orientation of Phe325 in subunit 1 were the same as in subunit 2, it would clash with Pro44 of the ordered cytochrome; thus, one effect of having the ordered cytochrome present in subunit 1 is to fix the orientation of Phe325 at the protein surface. In R289K-b_2 (before strict NCS constraints were introduced), Phe325 was found to protrude into solution in both subunits and had relatively high group B-factors, which was consistent with cytochrome disorder in both subunits.

For analysis of R289K-b_2, the best model for comparison is the recombinant sulfite adduct structure determined at 2.6 Å resolution (*6*). This is because sulfite is bound to the flavin N5 atom in both structures and is likely to have similar perturbing effects resulting from its negative charge and hydrogen-bonding propensity. In addition, both constructs lack the first five residues at the N-terminus of the native yeast protein, due to the makeup of the DNA used for expression (*3*), and both recombinant forms were crystallized from PEG rather than MPD. Except for the lysine substitution and the absence of both cytochrome domains in the R289K mutant protein, its structure is generally quite similar to that of the wild-type recombinant protein. The rms difference in C positions between them is 0.35, and there are no deviations greater than 1.0.

(3) Active Site. Four residues in the active site of flavocytochrome b_2, shown to be important for catalysis, are hydrogen-bonded to the sulfite ion in the recombinant enzyme structure (*6*). These are Tyr143, Tyr254, His373, and Arg376 (Figure 5a). The side chains of Tyr143 and Arg376 bind to the carboxylate of pyruvate (the product and substrate of the reverse reaction, respectively). Tyr254 is believed to form a hydrogen bond to the α-hydroxyl group of the substrate to stabilize the transition state (*38*), and His373 is the active site base during catalysis, assuming a carbanion mechanism (*39*). In R289K-b_2, these side chains are essentially in the same configuration as in the recombinant sulfite-bound structure, and all of the hydrogen bonds to sulfite are maintained. In the native yeast flavocytochrome

[4] The polypeptide segment from positions 298−320 is largely disordered in the native yeast structure of flavocytochrome b_2 (*5*).

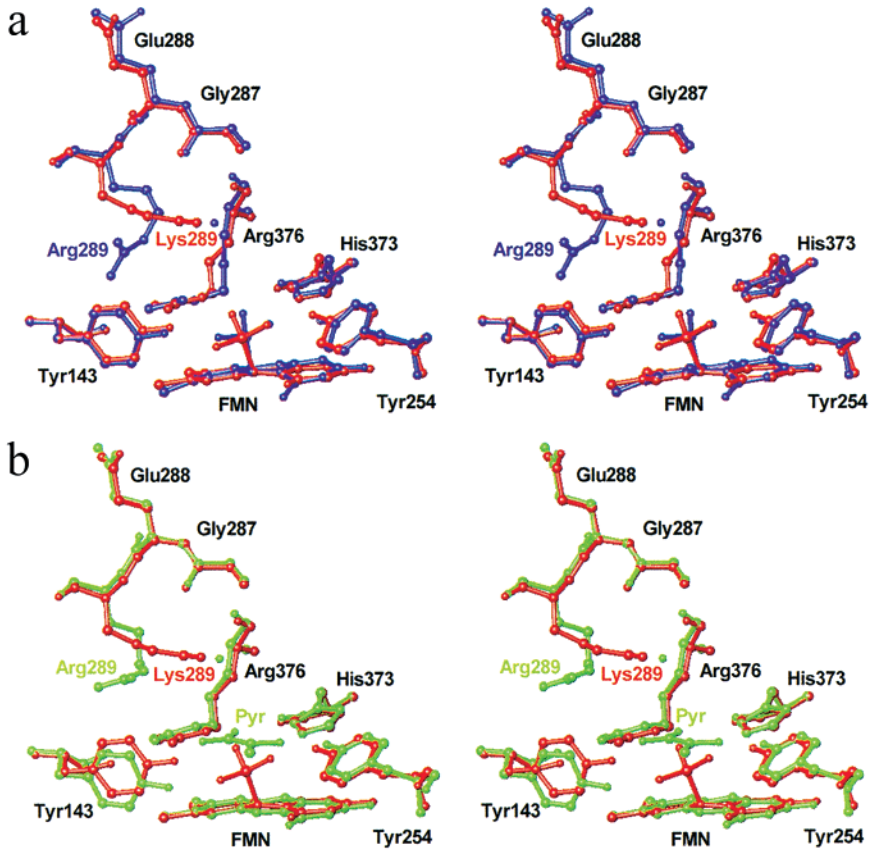

FIGURE 5: Stereoview of the active site residues (Tyr143, Tyr254, His373, and Arg376 and FMN) surrounding Arg/Lys289 in the R289K mutant, the recombinant wild-type sulfite adduct, and the native yeast flavocytochrome b_2. (a) R289K mutant (red) and recombinant sulfite adduct (blue). The sulfite adduct of FMN for both proteins is also shown. A water molecule in the wild-type recombinant enzyme structure displaced by the lysine side chain is shown in blue. (b) R289K mutant (red) and native yeast structure (green). The position of pyruvate, bound to the active site of subunit 2 of the native yeast enzyme structure, is also shown in green. The water molecule in the latter structure displaced by the lysine side chain is shown in green (see the text). This diagram was generated using TURBO-FRODO (*25*).

b_2 structure, where water or pyruvate is bound at the active site, His373 is in the same position as in the sulfite-containing structures. Conversely, Tyr143 and Tyr254 are each rotated away from their positions in the recombinant enzyme−sulfite adduct structures, differing in the positions of their hydroxyls on average by about 1.4 and 1.1 Å, respectively.

In R289K-b_2, the side chain of Lys289 is directed toward the active site (Figure 5). It is surrounded by four oxygen atoms, the peptide carbonyls of Gly287 (3.4 Å) and Arg376 (3.9 Å), the side chain carbonyl of Gln377 (3.7 Å), and a sulfite oxygen (4.6 Å). In the native yeast flavocytochrome b_2, Arg289 points away from the active site and forms a salt bridge with Asp292. In the recombinant sulfite-bound enzyme structure, Arg289 is discretely disordered. In half the molecules, it is oriented like it is in the yeast enzyme structure, but in the other half, it is directed toward the active site and forms a hydrogen bond to one of the oxygen atoms of the sulfite anion (*6*).[5]

DISCUSSION

As mentioned in the introductory section, the elucidation of the crystal structure of the recombinant flavocytochrome b_2−sulfite complex suggested a possible role for Arg289 in catalysis of lactate dehydrogenation. Interestingly, the effects of the minimal mutation of Arg to Lys, which have been probed both in solution and in the crystal, clearly indicate that, indeed, Arg289 has to be added to the list of catalytic residues.

In the crystal, Lys289 adopts a conformation roughly similar to the second conformation of Arg289 in the sulfite complex crystal structure (*6*),[5] namely, pointing toward the active site and displacing the same water molecule; however, as its side chain is shorter than that of an arginine, it does not interact directly with the sulfite anion, but appears to be close enough to exert an electrostatic influence. Superposition of the native yeast and R289K mutant enzyme structures (Figure 5b) indicates that the lysine NZ is about 3.9 Å from the pyruvate carboxylate; a similar superposition with lactate modeled into the native enzyme active site (*40*) gives the same indication, and with a slight movement of the lysine side chain, formation of a hydrogen bond to the substrate appears to be a reasonable possibility. Steady-state kinetics results, however, indicate that the energy of the Michaelis complex and that of the transition state are affected, the former by about 1 kcal/mol and the latter by 2.6 kcal/mol (Table 2). The stopped-flow results cannot be analyzed as precisely, considering that the values for the wild-type enzyme with the same buffer were obtained at 5 °C. The rationale for this situation is as follows. On one hand, the wild-type enzyme is too fast in phosphate buffer for stopped-flow studies at 30 °C. On the other hand, the mutant enzyme would be even slower at 5 °C than at 30 °C, and we feared

[5] The coordinates for the alternative conformation of the Arg289 side chain in the recombinant sulfite structure are available neither from the Protein Data Bank nor from the authors.

more serious complications than at 30 °C, due to the intersubunit electron reshuffling mentioned above. Stopped-flow values were determined before for the wild-type enzyme in Tris-HCl buffer (pH 7.5 and 25 °C) (*29*), but it appears to be preferable to compare data obtained under the same buffer conditions, with temperature as the only variable. It is classically assumed that a 10 °C increase in temperature induces a 2-fold increase in rate constants; if there is no significant affinity change with temperature, the comparison in Table 4 of the 30 °C k_{red}^{F}/K_d value (R289K-b_2) with the wild-type enzyme value at 5 °C yields a minimum estimate of 2.5−3 kcal/mol for the difference in transition-state energy for flavin reduction between wild-type and mutant enzymes. A similar comparison cannot be carried out for binding constants; indeed, as detailed in the Results, the flavin reduction traces reflect not only flavin reduction by the substrate but also a competition between reduction by the substrate and flavin reoxidation by intersubunit electron transfer; under these conditions, the significance of the K_d^{app} is in doubt. But the lactate K_M values derived from steady-state studies and the K_d value from stopped-flow analysis of heme reduction, which are similar, must be a good approximation of the K_d value, considering that flavin reduction is entirely limiting for heme reduction. Both parameters indicate a decrease in the level of Michaelis complex stabilization by at most 1 kcal/mol. Thus, all the kinetic data coincide in pointing to a stronger perturbation for the transition state in the mutant enzyme than for the Michaelis complex.

The crystal structure does not give a clear rationale for these changes. One could possibly invoke a difference in the electrostatic stabilization afforded by the localized charge of a lysine and the more diffuse one of the guanido group. In any case, the difference is felt more strongly on the transition state, for which the formation of the putative carbanionic intermediate requires a strong stabilization of the carboxylate negative charge so as to lower the pK_a of the Cα−H bond. It can therefore be proposed that Arg289 acts as an electrophilic center in conjunction with Arg376. In this respect, it is interesting to compare the effect of the R289K mutation to that of the Tyr143Phe mutation. The steady-state parameters for the Tyr143Phe mutant enzyme obtained with ferricyanide as an acceptor indicate that the loss of the hydroxyl group destabilizes both the Michaelis complex and the transition state by 1 kcal/mol in Tris buffer (*29*) and by 0.5−0.6 kcal/mol in phosphate buffer (*32*). Stopped-flow studies suggest an effect essentially on substrate binding. In other words, whereas both side chains take part in Michaelis complex stabilization, the integrity of the Arg289 side chain appears to be more important in catalysis than that of Tyr143.

Finally, the possibility that the proximity of the Lys289 positive charge to His373 may decrease the basicity of the latter cannot be excluded. It does not appear, however, that this could represent an important effect, since Arg289 in its alternative conformation would be expected to exert a similar effect. This idea could be tested by determining the pK_a of His373 using hydrogen exchange measurements during transhydrogenation reactions, as has been done for the wild-type enzyme and several mutant ones (*34*, *41*, *42*).

The consequence of the mutation with respect to phenyllactate dehydrogenation is less striking than for lactate (Table 3). For this poor substrate, it appears that the transition state is only slightly more destabilized than the Michaelis complex (1.5 vs 1.1 kcal/mol). We have similarly observed less deleterious effects on catalysis of phenyllactate oxidation than on lactate oxidation for some active site mutations at other positions (*35*).

Of the series of inhibitors tested, sulfite is the only one for which no affinity change is observed compared to the wild-type enzyme. This suggests that the inherent affinity of the sulfite ion for oxidized flavin, combined with its additional stabilization by hydrogen bonds and electrostatic interactions with Tyr143, Tyr254, $HisH^+373$, and Arg376 (*6*, *43*; see also Figure 5), overpowers any effects of the R289K mutation. D-Lactate and L-mandelate behave as pure competitive inhibitors for R289K-b_2, as they do for the wild-type enzyme. Their K_i values are somewhat higher, amounting to a loss in binding energy of 0.8−0.9 kcal/mol, corresponding essentially to the same destabilization as that of the Michaelis complex for lactate and phenyllactate.

The behavior of pyruvate and oxalate and the loss of inhibition by excess substrate are more unexpected. The complex behavior exhibited by pyruvate with respect to the wild-type enzyme (see the Results) can most probably be ascribed to the binding of this ligand to the E·FMN$^\bullet$ state (*44*, *45*). Similarly, inhibition by excess substrate originates from lactate having a weak affinity for the E·FMN$^\bullet$ state (*32*). As for oxalate, the origin of the mixed inhibition it exerts on the wild-type enzyme has never been studied in detail, but it probably also arises from its binding to the E·FMN$^\bullet$ state, and possibly to the E·FMN^- state as well, as discussed previously (*34*). Therefore, the facts that the inhibition by excess substrate is not observed and that pyruvate and oxalate are strict competitive inhibitors with respect to the mutant enzyme all suggest that these three compounds have lost affinity for the R289K-b_2 E·FMN$^\bullet$ state. Thus, the unexpected conclusion is that R289 also contributes to ligand binding at the active site when the flavin is in the semiquinone state, and that K289 cannot replace it, at least not efficiently. Finally, the K_d values that were determined spectrophotometrically for pyruvate and oxalate binding to the wild-type enzyme oxidized state are somewhat smaller than the competitive K_i values obtained for the mutant enzyme (Table 5), again indicating a role of the R289 guanido group in the binding of ligands to the oxidized enzyme.

With respect to steps of the catalytic cycle beyond flavin reduction, as discussed above, it appears probable that the first of these, namely, electron transfer from $FMNH^-$ to oxidized heme b_2 (Scheme 1, **2** to **3**), has not been altered by the mutation. Indeed, the heme reduction rate is entirely limited by flavin reduction, and the ferricyanide K_M value indicates that the external oxidant cannot compete with heme b_2 for electrons from $FMNH^-$ any more than in the wild-type enzyme. But the second intramolecular step, namely, electron transfer from FMN$^\bullet$ to oxidized heme b_2, may have been altered by the mutation. Indeed, the k_{red} values for heme and flavin reduction, about 28 s^{-1} (Table 4), are clearly higher than steady-state values for both ferricyanide and cytochrome *c* reduction (Table 2). In the presence of acceptors, the catalytic cycle comprises steps not observed in the stopped flow: with cytochrome *c*, for example, a one-electron transfer from FMN$^\bullet$ to heme b_2 (Scheme 1, **4** to **5**)

and two steps of electron transfer from reduced heme b_2 to oxidized heme *c* (**3** to **4** and **5** to **1**). Assuming that the transfer steps to cytochrome *c* remain as rapid in the mutant enzyme as they are in the wild-type one (*45*), the somewhat limiting step in the steady state for R289K-b_2 can be identified as the electron transfer from $FMN^{\bullet}$ to heme b_2 (Scheme 1, **4** to **5**). No estimate of this rate is available for the wild-type enzyme at the same temperature in phosphate buffer. It was determined to be 120 s^{-1}, at 25 °C in Tris-HCl buffer (pH 7.5) (*46*). Also, *T*-jump experiments in phosphate buffer suggested a value of 200 s^{-1} at 16 °C (*47*). Using this latter value and assuming that it would be at least doubled at 30 °C, one would expect steady-state and stopped-flow rates to be identical within error. The previously published data obtained in Tris-HCl buffer with R289K-b_2 (*28*), combined with the value of 120 s^{-1} quoted above (*46*), point to a similar conclusion. It would thus appear that the mutation might well have affected the second electron transfer step between flavin and heme, possibly through a redox potential modification.

The total absence of the heme domain in the R289K-b_2 crystal structure was unexpected. One explanation is that the weak water-mediated hydrogen bond between Arg289 and the heme propionate (*5*) does contribute to the stabilization of the domain in the crystalline state. Such stabilization would not appear to affect the interdomain electron transfer properties of the mutant in solution since the flavin to heme electron transfer rate is limited by the rate of flavin reduction by substrate. Other explanations include the limited resolution of the X-ray data and the generally high degree of thermal motion observed for other mutants of flavocytochrome b_2.

In conclusion, R289 is now identified as an additional active site residue in flavocytochrome b_2. It interacts with the substrate both in the ground state and in the transition state. It must play the role of an electrophilic center together with the previously identified R376; indeed, neutralization of the carboxylate negative charge must be particularly important, in view of the proposed carbanionic character of the transition state. R289 is strictly conserved in more than a dozen amino acid sequences of members of the family of α-hydroxy acid oxidizing enzymes. Its possible role in catalysis started being suspected when its alternative conformation was detected in the crystal structure of the recombinant flavocytochrome b_2−sulfite adduct (*6*). Recently, the crystal structure of glycolate oxidase in complex with several inhibitors showed a direct interaction between Arg164 (the homologue of flavocytochrome b_2 Arg289) and these compounds (*48*); this interaction would not have been predicted from the free enzyme crystal structure (*49*), where the Arg164 side chain stacks against Arg257 (the homologue of flavocytochrome b_2 R376) and forms an electrostatic interaction with invariant Asp167, as found originally for R289 in the native yeast enzyme structure (*5*). Furthermore, Arg187 of L-lactate monooxygenase, also a homologue of Arg289 in flavocytochrome b_2, has recently been mutagenized to Met and shown to be important for substrate binding and catalysis (*50*). It thus seems probable that this invariant residue plays a catalytic role in all family members.

REFERENCES

1. Daum, G., Böhni, P. C., and Schatz, G. (1982) *J. Biol. Chem. 252*, 13028−13033.
2. Appleby, C. A., and Morton, R. K. (1954) *Nature 173*, 749−752.
3. Black, M. T., White, S. A., Reid, G. A., and Chapman, S. K. (1989) *Biochem. J. 258*, 255−259.
4. Jacq, C., and Lederer, F. (1974) *Eur. J. Biochem. 41*, 311−320.
5. Xia, Z.-X., and Mathews, F. S. (1990) *J. Mol. Biol. 212*, 837−863.
6. Tegoni, M., and Cambillau, C. (1994) *Protein Sci. 3*, 303−313.
7. Lederer, F., and Mathews, F. S. (1987) in *Flavins and Flavoproteins* (Edmondson, D. E., and McCormick, D. B., Eds.) pp 133−142, Walter de Gruyter, Berlin.
8. Lindqvist, Y., Brändén, C. I., Mathews, F. S., and Lederer, F. (1991) *J. Biol. Chem. 266*, 3198−3207.
9. Dong, J. M., Taylor, J. S., Latour, D. J., Iuchi, S., and Lin, E. C. C. (1993) *J. Bacteriol. 175*, 6671−6678.
10. Giegel, D. A., Williams, C. H., Jr., and Massey, V. (1990) *J. Biol. Chem. 265*, 6626−6632.
11. Maeda-Yorita, K., Aki, K., Sagai, H., Misaki, H., and Massey, V. (1995) *Biochimie 77*, 631−642.
12. Lê, K. H. D., and Lederer, F. (1991) *J. Biol. Chem. 266*, 20877−20881.
13. Tsou, A. Y., Ransom, S. C., and Gerlt, J. A. (1990) *Biochemistry 29*, 9856−9862.
14. Illias, R. M., Sinclair, R., Robertson, D., Neu, A., Chapman, S. K., and Reid, G. A. (1998) *Biochem. J. 333*, 107−115.
15. Lederer, F., Belmouden, A., and Gondry, M. (1996) *Biochem. Soc. Trans. 24*, 77−83.
16. Kunkel, T. A. (1985) *Proc. Natl. Acad. Sci. U.S.A. 82*, 488−492.
17. Sambrook, J., Fritsch, E. F., and Maniatis, T. (1989) *Molecular Cloning: A Laboratory Manual*, 2nd ed., Cold Spring Harbor Laboratory Press, Cold Spring Harbor, NY.
18. Labeyrie, F., Baudras, A., and Lederer, F. (1978) *Methods Enzymol. 53*, 238−256.
19. Hazzard, J. T., Cusanovich, M. A., Tainer, J. A., Getzoff, E. D., and Tollin, G. (1986) *Biochemistry 25*, 3318.
20. Pompon, D., Iwatsubo, M., and Lederer, F. (1980) *Eur. J. Biochem. 104*, 479−488.
21. Capeillère-Blandin, C., Bray, R. C., Iwatsubo, M., and Labeyrie, F. (1975) *J. Biochem. 54*, 549−566.
22. Otwinowski, Z., and Minor, W. (1997) *Methods Enzymol. 276*, 307−326.
23. Brünger, A. T. (1992) *X-PLOR version 3.1. A system for crystallography and NMR*, Yale University Press, New Haven, CT.
24. Brünger, A. T., Adams, P. D., Clore, G. M., DeLano, W. L., Gros, P., Grosse-Kunstleve, R. W., Jiang, J. S., Kuszewski, J., Nilges, M., Pannu, N. S., Read, R. J., Rice, L. M., Simonson, T., and Warren, G. L. (1998) *Acta Crystallogr. D54*, 905−921.
25. Roussel, A., and Cambillau, C. (1991) TURBO-FRODO, in *Silicon Graphics Geometry Partners Directory 86*, Silicon Graphics, Mountain View, CA.
26. Lederer, F. (1978) *Eur. J. Biochem. 88*, 425−431.
27. Gondry, M., Lê, K. H. D., Manson, F. D. C., Chapman, S. K., Mathews, F. S., Reid, G., and Lederer, F. (1995) *Protein Sci. 4*, 925−935.
28. Pike, A. D., Chapman, S. K., Manson, F. D. C., Reid, G. A., Gondry, M., and Lederer, F. (1997) in *Flavins and Flavoproteins 1996* (Stevenson, K., Massey, V., and Williams, C. H., Eds.) University of Calgary Press, Calgary, AB.
29. Miles, C. S., Rouvière-Fourmy, N., Lederer, F., Mathews, F. S., Reid, G. A., Black, M. T., and Chapman, S. K. (1992) *Biochem. J. 285*, 187−192.
30. Iwatsubo, M., Mevel-Ninio, M., and Labeyrie, F. (1977) *Biochemistry 16*, 3558−3566.
31. Balme, A., Brunt, C. E., Pallister, R., Chapman, S. K., and Reid, G. A. (1995) *Biochem. J. 309*, 601−605.
32. Rouvière, N., Mayer, M., Tegoni, M., Capeillère-Blandin, C., and Lederer, F. (1997) *Biochemistry 36*, 7126−7135.

33. Pompon, D. (1980) *Eur. J. Biochem. 106*, 151−159.
34. Gondry, M., and Lederer, F. (1996) *Biochemistry 35*, 8587−8594.
35. Gondry, M. (1994) Thèse de l'Université Paris XI, Université Paris XI, Paris.
36. Cornish-Bowden, A. (1974) *Biochem. J. 137*, 143−144.
37. Laskowski, R. A., MacArthur, M. W., Moss, D. S., and Thornton, J. M. (1993) *J. Appl. Crystallogr. 26*, 283−291.
38. Dubois, J., Chapman, S. K., Mathews, F. S., Reid, G. A., and Lederer, F. (1990) *Biochemistry 29*, 6393−6400.
39. Lederer, F. (1991) Flavocytochrome b_2, in *Chemistry and Biochemistry of the Flavoenzymes* (Müller, F., Ed.) Vol. 2, pp 153−242, CRC Press, Boca Raton, FL.
40. Lederer, F. (1991) in *Flavins and Flavoproteins 1990* (Curti, B., Ronchi, S., and Zanetti, G., Eds.) pp 773−782, Walter de Gruyter, Berlin.
41. Balme, A., and Lederer, F. (1994) *Protein Sci. 3*, 109−117.
42. Rao, K. S., and Lederer, F. (1998) *Protein Sci. 7*, 1531−1537.
43. Tegoni, M., and Mathews, F. S. (1988) *J. Biol. Chem. 263*, 19278−19281.
44. Tegoni, M., Janot, J.-M., and Labeyrie, F. (1990) *Eur. J. Biochem. 190*, 329−342.
45. Daff, S., Sharp, R. E., Short, D. M., Bell, C., White, P., Manson, F. D. C., Reid, G. A., and Chapman, S. K. (1996) *Biochemistry 35*, 6351−6357.
46. Daff, S., Ingledew, W. J., Reid, G. A., and Chapman, S. K. (1996) *Biochemistry 35*, 6345−6350.
47. Tegoni, M., Silvestrini, M. C., Guigliarelli, B., Asso, M., Brunori, M., and Bertrand, P. (1998) *Biochemistry 37*, 12761−12771.
48. Sternberg, K., and Lindqvist, Y. (1997) *Protein Sci. 6*, 1009−1115.
49. Lindqvist, Y., and Brändén, C.-I. (1989) *J. Biol. Chem. 264*, 3624−3628.
50. Sanders, S. A., Williams, C. H., Jr., and Massey, V. (1999) *J. Biol. Chem. 274*, 22289−22295.
51. Kleywegt, G. J., and Brünger, A. T. (1996) *Structure 4*, 897−904.

BI9925975